Effects of Long- and Short-Term Atmospheric Water Cycles on the Water Balance over the Maritime Continent

HIRONARI KANAMORI

Institute for Space-Earth Environmental Research, Nagoya University, Nagoya, Japan

TOMO'OMI KUMAGAI

Graduate School of Agricultural and Life Sciences, University of Tokyo, Tokyo, and Institute for Space-Earth Environmental Research, Nagoya University, Nagoya, Japan

HATSUKI FUJINAMI AND TETSUYA HIYAMA

Institute for Space-Earth Environmental Research, Nagoya University, Nagoya, Japan

TETSUZO YASUNARI

Research Institute for Humanity and Nature, Kyoto, Japan

(Manuscript received 24 March 2018, in final form 1 July 2018)

ABSTRACT

This study investigated atmospheric water cycles over several time scales to understand the maintenance processes that control heavy precipitation over the islands of the Maritime Continent. Large island regions can be divided into land, coastal, and ocean areas based on the characteristics of both the hydrologic cycle and the diurnal variation in precipitation. Within the Maritime Continent, the major islands of Borneo and New Guinea exhibit different hydrologic cycles. Large-scale circulation variations, such as the seasonal cycle and the Madden–Julian oscillation, have a lesser effect on the hydrologic cycle over Borneo than over New Guinea because the effects depend on their shapes and locations. The impact of diurnal variations on both regional-scale circulation and water exchange between land and coastal regions is pronounced over both islands. The recycling ratio of precipitation, which can be related to stronger diurnal variation in the atmospheric water cycle that results from enhanced evapotranspiration over tropical rain forests, is higher over Borneo than over New Guinea.

1. Introduction

The Maritime Continent (MC) is an archipelago in Southeast Asia that comprises large islands such as New Guinea, Borneo, and Sumatra. This shallow-ocean environment contains many islands and lies within a tropical warm pool (Ramage 1968). The major islands of the MC are characterized by heavy precipitation because the topography generates localized convection that leads to the formation of active cloud/precipitation systems (e.g., Neale and Slingo 2003; Biasutti et al. 2012). Convective cloud systems over the MC release considerable latent heat that constitutes a major component of the atmospheric heat budget. In addition, thermal land–sea contrasts associated with the major islands in this warm ocean environment generate complex local circulations that play important roles in both the energy cycle and the hydrologic cycle of the MC (Neale and Slingo 2003).

Temporal variations in convection and precipitation exhibit pronounced diurnal and intraseasonal variabilities, and large-scale processes such as the Madden–Julian oscillation (MJO; Madden and Julian 1994) play important roles in the intraseasonal variability over the MC (Ichikawa and Yasunari 2007; Rauniyar and Walsh 2011; Kanamori et al. 2013). The atmospheric water cycle also shows significant regional variations at seasonal, intraseasonal, and diurnal time scales (Ruane and Roads 2008). Diurnal convection and precipitation cycles are controlled by thermal contrasts between land

Corresponding author: Hironari Kanamori, kanamori@isee.nagoya-u.ac.jp

DOI: 10.1175/JHM-D-18-0052.1

and ocean surfaces that induce land–sea breeze circulations (Houze et al. 1981; Yang and Slingo 2001; Kikuchi and Wang 2008). The characteristics of the diurnal precipitation cycle have been described for the main islands in the MC, that is, Sumatra, Borneo, and New Guinea (Mori et al. 2004; Ichikawa and Yasunari 2006, 2008; Kanamori et al. 2013). The diurnal convection cycle of the MC is characterized by convection peaks from late afternoon to evening over land and from nighttime to morning over the surrounding ocean regions (e.g., Ohsawa et al. 2001; Yang and Slingo 2001; Kikuchi and Wang 2008; Biasutti et al. 2012).

The MJO is also a dominant mode of deep convection and heavy precipitation over the MC. The modulation of the diurnal convection/precipitation cycle by the MJO has been investigated in many previous studies (e.g., Chen and Takahashi 1995; Ichikawa and Yasunari 2006, 2008; Tian et al. 2006; Rauniyar and Walsh 2011; Kanamori et al. 2013). Using hourly precipitation data from a dense array of stations, Kanamori et al. (2013) showed that the MJO has a stronger effect on the diurnal precipitation cycle in coastal areas compared with interior regions of west Borneo. The features of propagating convective cloud systems over Borneo and New Guinea related to the MJO have been described using Tropical Rainfall Measuring Mission (TRMM) datasets (Ichikawa and Yasunari 2006, 2008). These studies revealed that the effect of large-scale circulation change on propagating convective systems differed between islands. Although these previous studies focused on the relationship between diurnal convection/precipitation and large-scale circulation (i.e., the MJO) over the MC, the processes that deliver heavy precipitation over land remain poorly understood.

Deep convection and heavy precipitation throughout the year create a major moisture sink in the MC. Atmospheric water budget analyses over the MC show that moisture flux convergence variability contributes to precipitation variability on the MJO time scale (Chen et al. 1995). In addition, Waliser et al. (2009) used satellite data to show that increasing (decreasing) precipitation is maintained by the preceding moisture flux convergence (divergence) on MJO time scales and that the contribution of evaporation to precipitation is relatively small.

Tropical rain forests represent a major source of global and regional hydrologic fluxes (Aragão 2012), and evapotranspiration over land might also play a major role in the hydrologic cycle of the MC. For example, estimates from ground-based observations suggest that the contribution of evapotranspiration to annual precipitation ranges from about 50% (Kume et al. 2011) to 74% (Kumagai et al. 2005) in western Borneo. In contrast, a study based on a general circulation model suggested that water recycling is not significant in Borneo (Goessling and Reick 2011). Kumagai et al. (2013) showed that the climatological annual mean moisture flux convergence over Borneo made little contribution to total rainfall despite heavy precipitation throughout the year. Conversely, for other major islands (e.g., New Guinea), moisture flux convergence was found to make a considerable contribution to precipitation. Thus, it must be assumed that the hydrologic cycle is different for each island (Kumagai et al. 2013). Furthermore, forest cover change might also modify the climate and the hydrologic cycle at regional and global scales. Evapotranspiration from forests has the capacity to modify precipitation and, in turn, alter the regional water balance (Kanae et al. 2001; Yasunari et al. 2006; Bonan 2008; Spracklen et al. 2012). Therefore, a water budget analysis must be conducted separately for complex land and ocean areas such as the MC.

To understand better the processes responsible for heavy precipitation as part of the hydrologic cycle, this study estimated the land and ocean atmospheric water budget over the MC. The impact of large-scale circulation on the diurnal precipitation cycle differs between the major islands of the MC; therefore, it was necessary to calculate the water budget for each island separately. This work focused on New Guinea and Borneo, which are the largest and the second-largest islands in the region, respectively. Section 2 describes the methods used to calculate the atmospheric water budget, and section 3 describes the datasets used in the analysis. Section 4 examines both seasonal and intraseasonal variations in the hydrologic cycle of the MC associated with the MJO, together with the features of the diurnal hydrologic cycle. Finally, a discussion and our conclusions are provided in section 5.

2. Methods

The atmospheric water budget equation (Trenberth and Guillemot 1995) can be written as

$$\left\langle \frac{\partial W}{\partial t} \right\rangle + \nabla \cdot \langle \mathbf{Q} \rangle = \langle E - P \rangle , \tag{1}$$

where W is precipitable water content ($\mathrm{kg\,m^{-2}}$), t is time (s), E is evaporation and evapotranspiration ($\mathrm{kg\,m^{-2}\,s^{-1}}$), P is precipitation ($\mathrm{kg\,m^{-2}\,s^{-1}}$), and $\mathbf{Q}$ is the vertically integrated moisture flux vector ($\mathrm{kg\,m^{-1}\,s^{-1}}$), where its convergence C ($\mathrm{kg\,m^{-2}\,s^{-1}}$) is given by $-\nabla \cdot \mathbf{Q}$.

The angled brackets denote the area average. Here, W and $\mathbf{Q}$ are given by

$$W = \frac{1}{g}\int_{p_t}^{p_s} q\, dp \quad \text{and} \tag{2}$$

$$\mathbf{Q} = \frac{1}{g}\int_{p_t}^{p_s} q\mathbf{V}\, dp, \tag{3}$$

where g is the acceleration due to gravity ($\mathrm{m\,s^{-2}}$); p_t and p_s are the pressure (Pa) at the top of the atmosphere and at the surface, respectively; q is specific humidity ($\mathrm{kg\,kg^{-1}}$), and $\mathbf{V}$ is the horizontal wind vector ($\mathrm{m\,s^{-1}}$). Vertical integration is performed from p_t (100 hPa) to the ground (surface pressure level). The local water use ratio (LWUR; %) is also defined from Eq. (1) as follows:

$$\mathrm{LWUR} = \frac{1}{\langle P\rangle}\left(\langle P\rangle + \left\langle\frac{\partial W}{\partial t}\right\rangle - \langle C\rangle\right)\times 100\,. \tag{4}$$

The LWUR is computed using area averages for each term in Eq. (1) in specific regions, and it represents the fraction of P in a region sustained by local E within the same region. For example, a small value of LWUR indicates that P is largely maintained by moisture convergence, while a large LWUR value indicates that local E dominates the precipitation recycling.

In this study, we focused on the MJO and the diurnal time scales of the hydrologic cycle over the MC because such time scales are known to be dominant in precipitation variability (Kanamori et al. 2013). Thus, we adopted the simple local moisture feedback strength (i.e., the LWUR) to investigate the smaller temporal and spatial scales of moisture feedback over the MC. This approach differed from that of van der Ent and Savenije (2011), which revealed the longer time scale of moisture feedback over the MC using the length and time scales based on global scales.

3. Datasets

The vertically integrated moisture flux convergence C and precipitable water content W are computed for 6-h intervals in the Japanese 25-year (1979–2004) reanalysis (JRA-25)/Japan Meteorological Agency Climate Data Assimilation system (JCDAS) on a 1.25° latitude–longitude grid (Onogi et al. 2007). The JRA-25/JCDAS dataset covers the period 1979–2013. The JRA-25/JCDAS assimilates the observational horizontal wind and specific humidity data throughout the troposphere. These reanalysis data can provide detailed and accurate information on the atmospheric water cycle over the MC, including complex land–ocean distributions that cannot be discerned in other coarse reanalysis data. This study used the JRA-25/JCDAS from 1998 to 2012 (15 years).

The TRMM PR 2A25 version 7 data (Iguchi et al. 2000) for the period 1998–2012 (15 years) were also used because the above reanalysis data did not assimilate the precipitation observations sufficiently. We compiled the TRMM PR data (orbital data with horizontal resolution of ~5 km) into gridded data with resolution of 0.15° × 0.15°. We used the near-surface rain rate to examine the spatial distribution of precipitation over the MC. The TRMM PR data with 1.25° × 1.25° resolution, which is same resolution as the reanalysis data, were also used to calculate P for the atmospheric water budget. Here, it should be noted that a combination of the reanalysis data and the precipitation observation data was used for estimating the atmospheric water budget components in Eq. (1).

The phase and amplitude of the MJO were defined according to the Real-Time Multivariate MJO (RMM) index (Wheeler and Hendon 2004). This index is based on a pair of empirical orthogonal functions of the combined 850-hPa zonal wind, 200-hPa zonal wind, and satellite-observed outgoing longwave radiation data averaged across the equator (15°N–15°S). The pair of principal component time series, which have the annual cycle and interannual variability components removed, are called RMM1 and RMM2, respectively. Here, eight MJO phases are defined by RMM1 and RMM2. Phases denote the period when the center of convective activity (i.e., low-level convergence) is located near Africa (phase 1), over the Indian Ocean (phases 2 and 3), over the MC (phases 4 and 5), over the western Pacific (phases 6 and 7), and over the eastern Pacific (phase 8).

4. Results

a. *Seasonal changes in precipitation and moisture flux convergence*

Figure 1 shows the climatological means (1998–2012) of precipitation and atmospheric circulation fields for boreal summer [May–September (MJJAS)] and winter [November–March (NDJFM)] over the MC. High values of precipitation are observed over the Indian Ocean, Indian subcontinent, Bay of Bengal, Indochina Peninsula, and South China Sea, which are related to the southwesterly wind at 850 hPa in MJJAS (Fig. 1a). Conversely, precipitation is enhanced over Sumatra, Borneo, and New Guinea in NDJFM (Fig. 1c). Moisture flux convergence corresponds to precipitation activity in both seasons (Figs. 1b,d). It should be noted that the stronger precipitation with the higher moisture flux convergence over New Guinea might be associated with

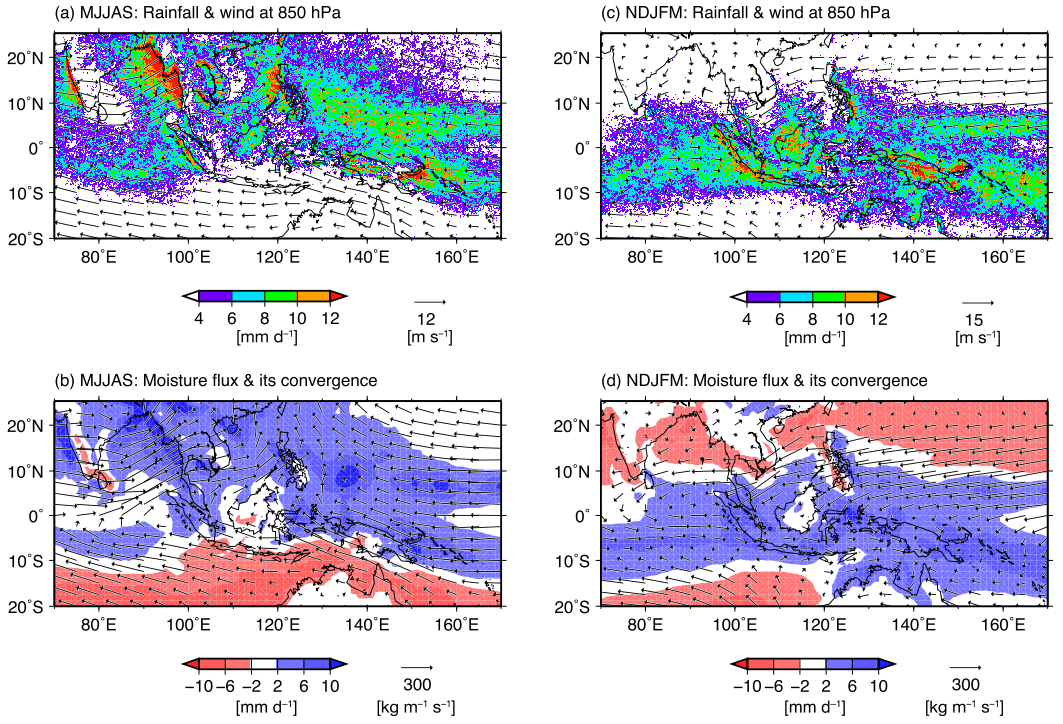

FIG. 1. Climatological (1998–2012) mean distributions of (a) TRMM-PR precipitation (mm day^{-1}; shaded areas) and wind vectors (m s^{-1}) at 850 hPa and (b) vertically integrated moisture (from the surface to 100 hPa) flux vectors (kg m^{-1} s^{-1}) and its convergence (mm day^{-1}; shaded areas) in boreal summer (MJJAS). (c),(d) As in (a) and (b), but in boreal winter (NDJFM).

its position close to the South Pacific convergence zone (SPCZ) in NDJFM. High values of precipitation are observed throughout the year in the MC, and precipitation centers tend to form over land rather than over oceans. In boreal winter, precipitation is enhanced, particularly over the west coast of Sumatra and over the mountain regions in both Borneo and New Guinea.

The spatial pattern of moisture flux convergence corresponds well with that of precipitation over the MC in the both seasons, except over Borneo. In the Borneo region, including the land and its surrounding ocean, moisture flux convergence in both seasons is very weak despite pronounced precipitation. In other words, the contribution of moisture flux convergence to precipitation can be assumed small over Borneo, which implies the impact of large-scale circulation (e.g., the seasonal cycle) on precipitation over Borneo is less than for other regions of the MC.

To investigate the contribution of the diurnal precipitation cycle to total precipitation variation over the MC, the percentage of total variance explained by the diurnal cycle was calculated using 3-h precipitation from the TRMM 3B42 version 7 data (Huffman et al. 2007) by dividing the mean diurnal cycle variance by the total variance including a more than 3-h time scale. A high percentage of the variance explained by the diurnal cycle (i.e., >64%) extends from islands to surrounding oceans in both seasons (Fig. 2). This index shows weak seasonal change between land and coastal regions (not figure shown). The annual mean of the percentage of total variance explained by the diurnal cycle is ~74% over the major MC islands and >64% over the surrounding oceans within ~400 km of the coast. The percentage of total variance is relatively small (<64%) over ocean areas more than 400 km from land in the MC. The percentage of the total variance explained by the diurnal cycle of moisture flux convergence is also higher over land and the surrounding oceans. Therefore, the spatial characteristics of the atmospheric water cycle of the MC can be distinguished based on the distribution of the percentage of total variance explained by the diurnal cycle.

The annual mean of the percentage of total variance explained by the diurnal precipitation cycle is calculated to classify the atmospheric water cycle more objectively. The threshold value of this percentage was defined as 66% to categorize domains for the water cycle (e.g., land and ocean). This was done so that our domains would be consistent with the definitions used in previous studies based on empirical orthogonal

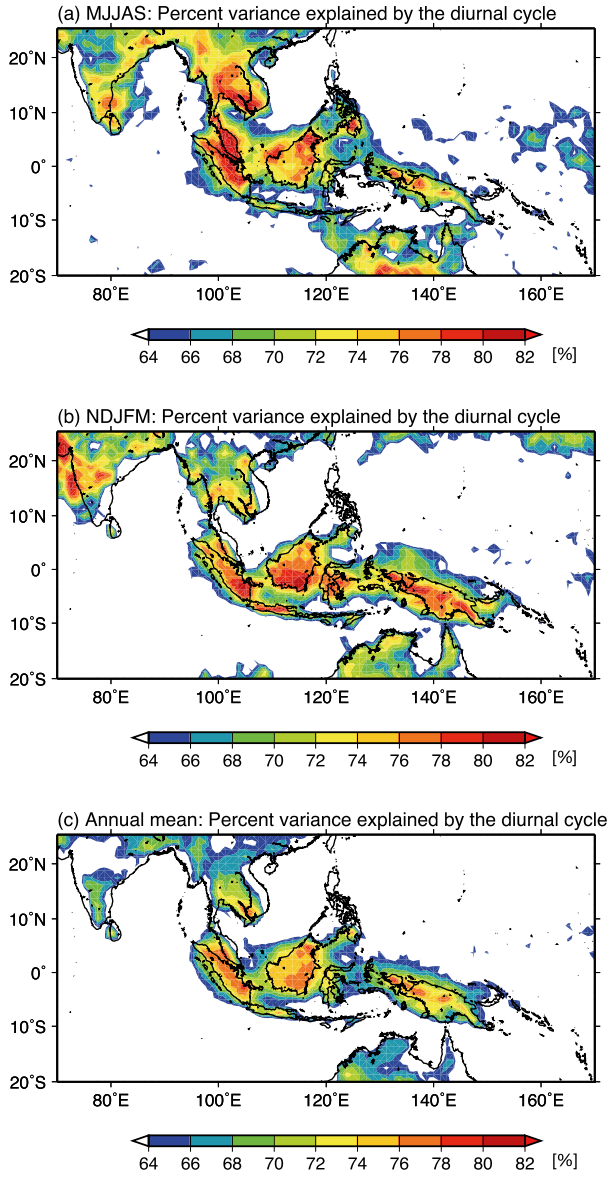

FIG. 2. Climatological (1998–2012) mean distribution of the percentage (%) of total variance explained by the diurnal cycle of precipitation from TRMM 3B42 precipitation in (a) MJJAS, (b) NDJFM, and (c) annual mean.

function analysis for the diurnal cycle of precipitation (Kikuchi and Wang 2008; Rauniyar and Walsh 2011). Figure 3 shows the domains determined for the atmospheric water budget analysis based on the percentage variance of the diurnal precipitation cycle over the MC. These domains are defined as the Borneo region (BO), New Guinea region (NG), and MC ocean region (MCO). Additionally, BO and NG are divided further into land regions (BOL and NGL), based on the land–ocean mask data of JRA-25/JCDAS, and coastal regions (BOC and NGC).

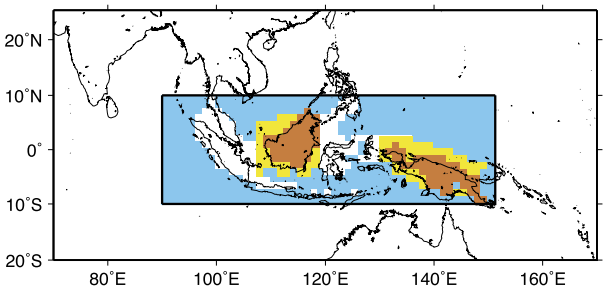

FIG. 3. Three computational domains used for examining the atmospheric water budget. The brown color indicates Borneo (BOL) and New Guinea (NGL), as defined using the land–ocean mask data of JRA-25/JCDAS. The yellow color shows coastal regions around both islands (BOC and NGC) defined as domains with >66% of the annual mean percentage of the total variance explained by the diurnal precipitation cycle. The blue shading shows the Maritime Continent ocean (MCO) region.

b. *Seasonal cycle of the regional atmospheric water budget*

Figure 4 shows the climatological monthly P, C, water vapor storage term, and the LWUR for each domain. The temporal change in precipitable water content W shows little variation and it is negligible compared with other components. Parameters P and C show similar variations over all domains. The seasonal cycles of P and C in BOL and BOC, exhibiting relatively higher values in November–January, can be associated with their enhancement by the northeasterly monsoon flow over BO in boreal winter (see Fig. 1). In BOL, the maximum values of P and C appear in November and October, respectively (Fig. 4a), while in BOC, the maximum values of both P and C appear in December (Fig. 4c). However, in NGL and NGC, both P and C peak in March (Figs. 4b,d). This might be consistent with the seasonal north–south migration of the intertropical convergence zone (ITCZ) over the MC and with the evolution of the SPCZ over a widespread area of the equatorial southern Pacific in NDJFM (Chang et al. 2005b; Ichikawa and Yasunari 2008). It is interesting to note that the strength of the seasonality of both P and C for all domains in Fig. 4 depends on the combined effects of large-scale circulations, for example, the positions of both the ITCZ and the SPCZ, and the northeasterly winter monsoon.

The contribution of C to P over land is smaller in BOL than in NGL throughout the year, and the contribution of C to P is higher over coastal areas (BOC and NGC) than over land (BOL and NGL; Fig. 4). The difference between P and C is similar throughout the year in all domains. Thus, the seasonal LWUR cycle shows smaller variation than the P and C cycles.

The LWUR is generally higher in BOL than NGL. In BOL and NGL, it increases to approximately 100% and

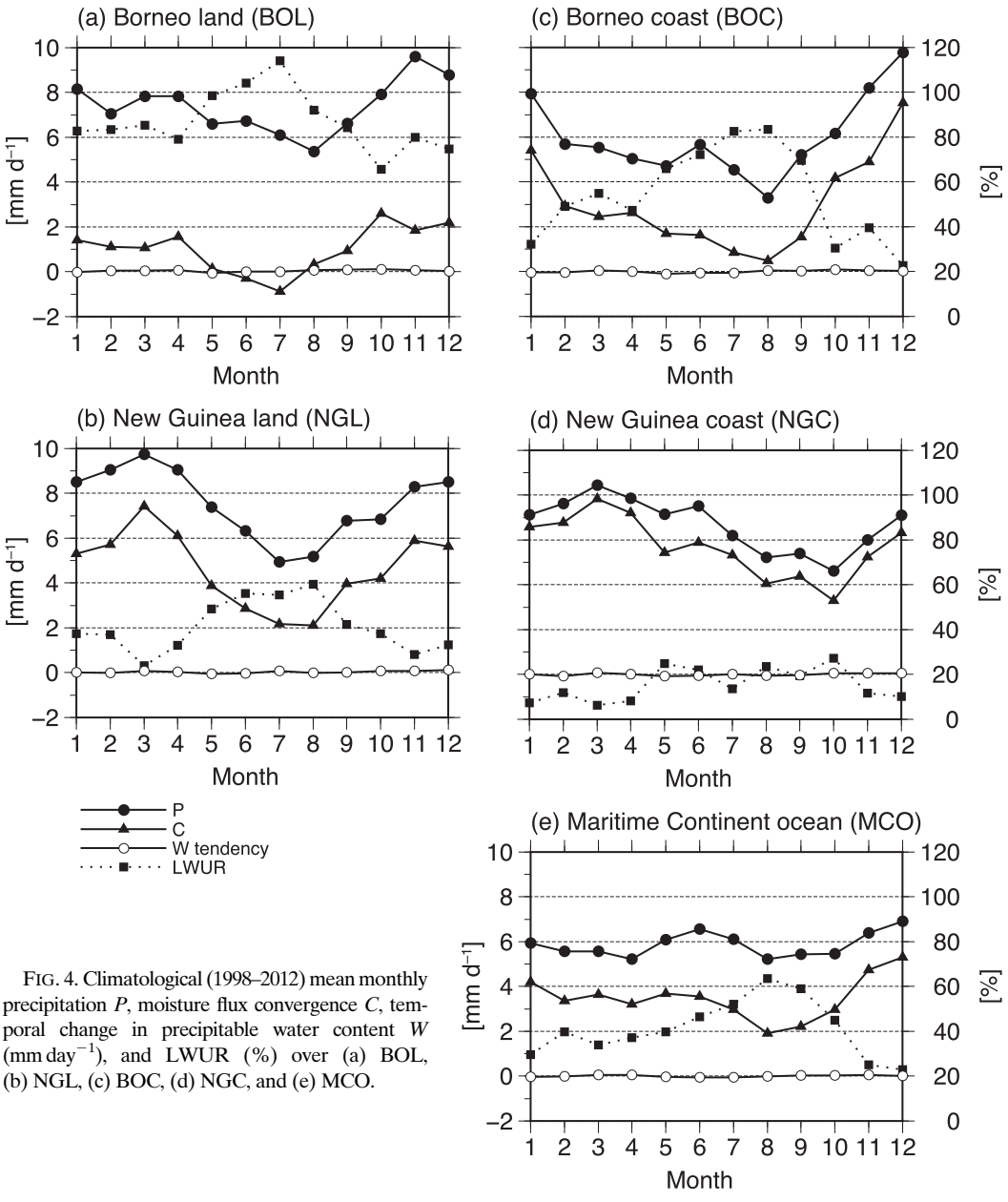

FIG. 4. Climatological (1998–2012) mean monthly precipitation P, moisture flux convergence C, temporal change in precipitable water content W (mm day^{-1}), and LWUR (%) over (a) BOL, (b) NGL, (c) BOC, (d) NGC, and (e) MCO.

45%, respectively, in boreal summer, whereas it decreases to approximately 80% and 25%, respectively, in boreal winter (Figs. 4a,b). The annual mean LWUR over BOL and NGL reaches up to 85% and 35%, respectively. Here, we should note that the LWUR represents not only the contribution of evapotranspiration to P but also the sensitivity to C when P is small, such as in the cases of BOC and NGC (Figs. 4c,d). Parameter C is stronger over coastal regions than over inland regions for both NG and BO; thus, the LWUR is larger over the islands than the surrounding oceans. The annual mean LWUR also differs between the MCO and coastal regions (BOC and NGC), that is, ~38%, 50%, and 12% in MCO, BOC, and NGC, respectively (Figs. 4c–e).

c. *Impact of MJO on the atmospheric water budget during boreal winter over the MC*

Deep convection and heavy precipitation over both NG and BO are enhanced in boreal winter (Chang et al. 2005a; Zhou and Wang 2006; Ichikawa and Yasunari 2008). Precipitation and convection over the MC are also affected by the MJO in this season (Hsu and Lee 2005; Hidayat and Kizu 2010). For example, the impact of the MJO on the seasonal variation of precipitation is

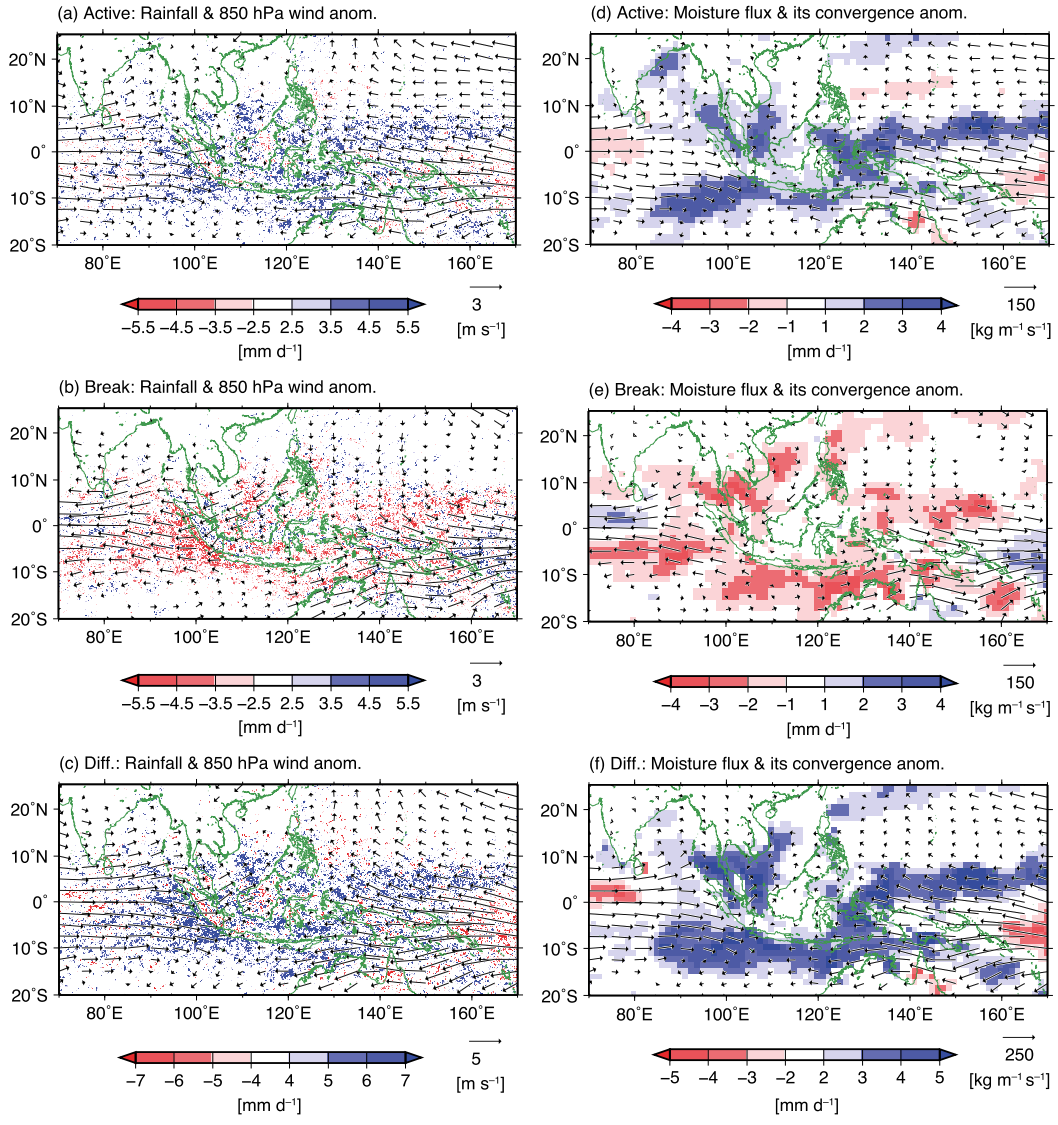

FIG. 5. Composite anomalies of daily precipitation (mm day^{-1}; shaded areas) and wind vectors (m s^{-1}) at 850 hPa in (a) active and (b) break phases and (c) the difference from active to break phases of the MJO. These anomalies are the difference from the boreal winter (NDJFM) mean. (d)–(f) As in (a)–(c), but for anomalies of vertically integrated moisture flux vectors (kg m^{-1} s^{-1}) and convergence (mm day^{-1}; shaded areas). Vectors and moisture flux convergence are plotted only if significant at the 95% confidence level.

relatively weak over the BO (e.g., Kanamori et al. 2013), while the MJO transits the Southern Hemisphere near the NG in boreal winter, resulting in the seasonal cycle of precipitation. Thus, here we focus on atmospheric water budget analyses for heavy precipitation over the MC in boreal winter. In the MC during boreal winter, the active (break) phases of the MJO are defined by phases 3–5 (phases 7–8 and 1) of the MJO index.

Figure 5 shows precipitation, anomalies of 850-hPa wind vectors, vertically integrated moisture flux vectors, and convergence in active and break periods during boreal winter. During the active period, precipitation is enhanced over the ocean of the MC. In the break period, precipitation tends to decrease over the ocean. The difference in precipitation between the two periods is larger over the ocean and coastal regions compared with land regions. The moisture flux convergence increases (decreases) over ocean regions during the active (break) period of the MJO; however, such an effect is not clear over BO and NG (Fig. 5). In other words, the variations in moisture flux convergence between active and break phases show little intraseasonal difference over BO and NG.

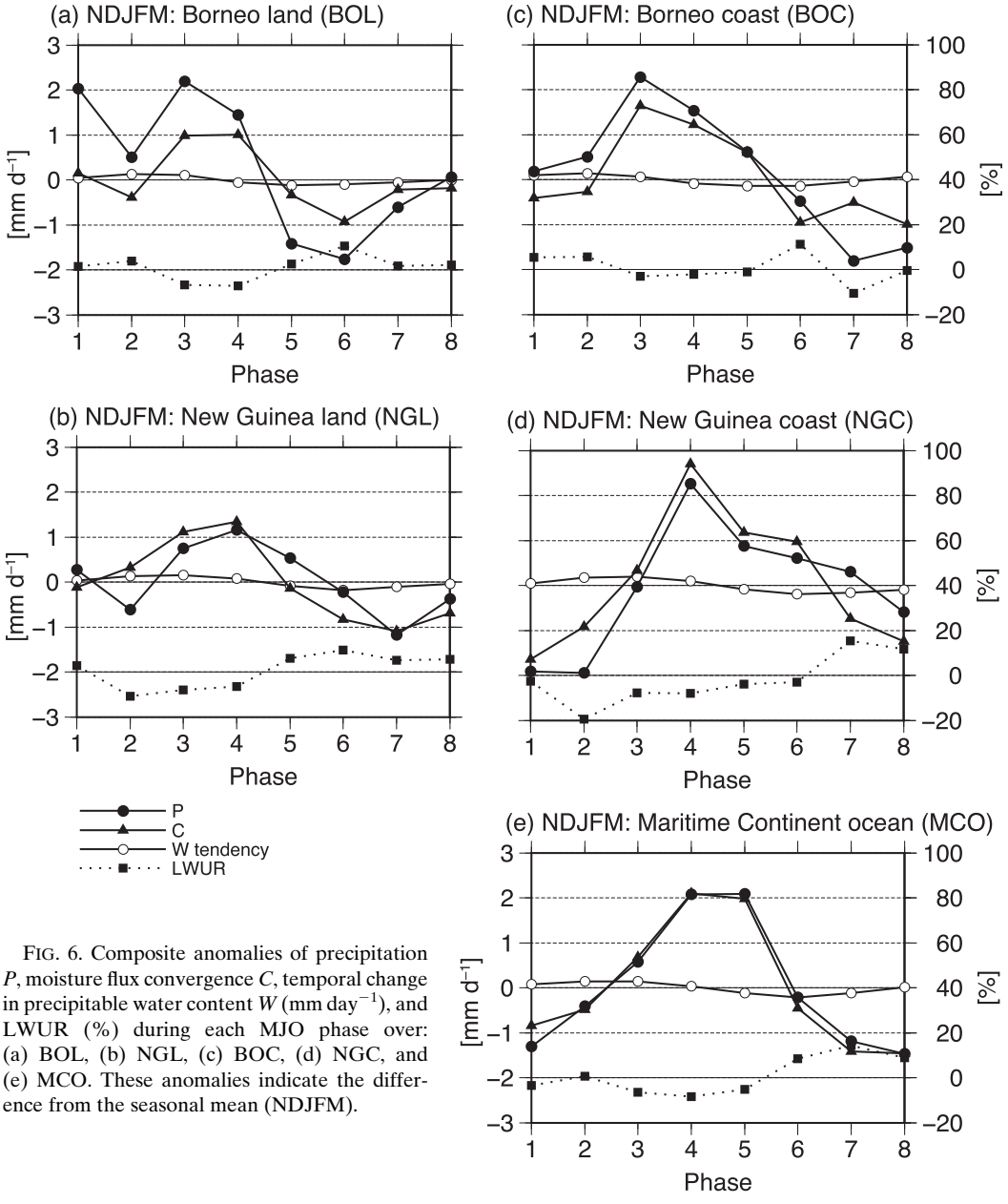

FIG. 6. Composite anomalies of precipitation P, moisture flux convergence C, temporal change in precipitable water content W (mm day^{-1}), and LWUR (%) during each MJO phase over: (a) BOL, (b) NGL, (c) BOC, (d) NGC, and (e) MCO. These anomalies indicate the difference from the seasonal mean (NDJFM).

Figure 6 shows the time evolution of the water budget component anomalies, which is the difference from the NDJFM mean in each MJO phase over the five domains in Fig. 3. Over all domains, P and C anomalies associated with the passage of the MJO are generally larger for phases 3–5 (active phases over the MC) and smaller for phases 7–1 (break phases over the MC). Although the center of convection is located over the Indian Ocean during phase 3 (see Wheeler and Hendon 2004), low-level easterly wind anomalies were enhanced over Borneo because easterly wind anomalies occur from the MC to the center of convection over the Indian Ocean (Wu and Hsu 2009). Therefore, the precipitation over Borneo starts to increase in advance of that over the MC. We should also note that the speed of propagation also becomes slower over the MC and the west Pacific compared with other longitudes (Hendon and Salby 1994). The water vapor storage term is unaffected by the MJO, and the variation of LWUR anomalies with MJO phase is also small. This suggests that the MJO has little effect on the LWUR compared with its effect on the P and C anomalies. For both BO and NG, P and C anomalies are larger over coastal regions (BOC and NGC) than over land (BOL and NGL) during active

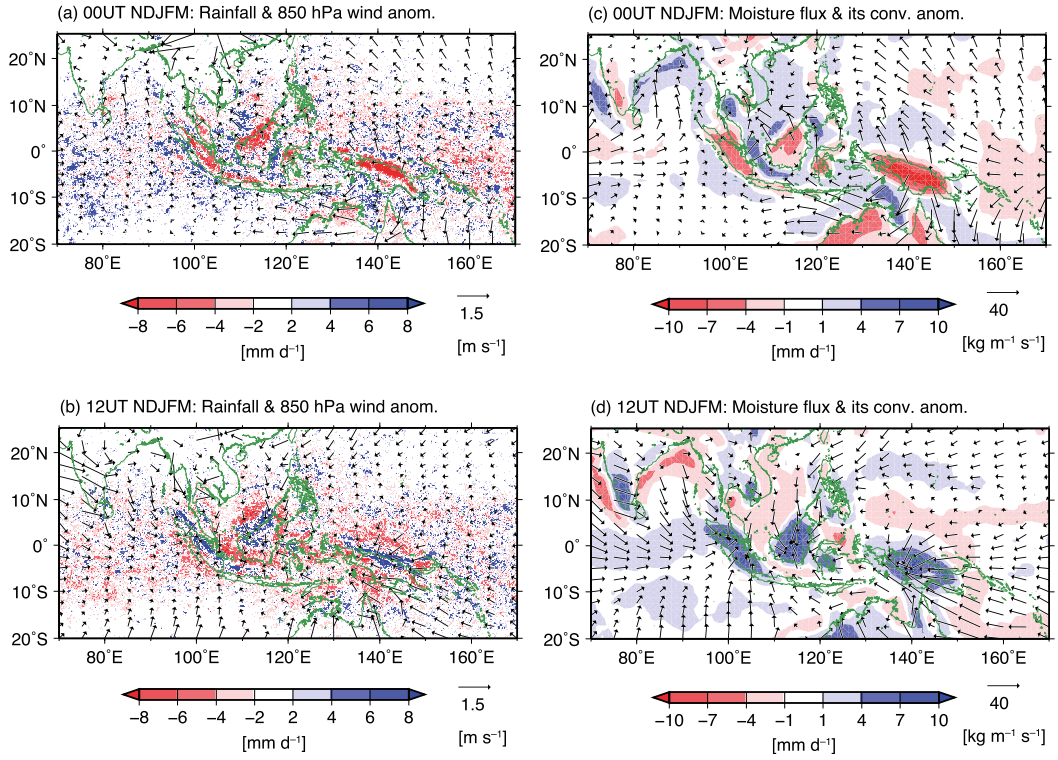

FIG. 7. (a),(b) Climatological (1998–2012) mean anomalies of TRMM-PR precipitation (mm day^{-1}; shaded areas) and wind vectors (m s^{-1}) at 850 hPa at 0000 UTC and 1200 UTC in NDJFM. (c),(d) As in (a) and (b), but for vertically integrated moisture flux vectors (kg m^{-1} s^{-1}) and convergence (mm day^{-1}; shaded areas). The climatological daily mean at each grid point has been removed.

periods. Parameter P increases more over the MCO than over other domains, and this is related to the rate of change from break to active periods.

The effect of the MJO on the water budget components varies from region to region. Over land, P and C are affected less by the MJO than over coastal regions and the MCO. The variation in P associated with the MJO coincides with the variation in C over all domains. However, the LWUR is influenced less on the MJO time scale in all of the domains. Therefore, MJO-induced changes in large-scale circulation can affect the fluctuations in P and C, which have greater variation over coastal regions (BOC and NGC) and the MCO than over land (BOL and NGL). However, the contribution of local-scale effects (i.e., evaporation) on P is influenced less by the MJO.

d. Effect of diurnal variations on the atmospheric water cycle during the boreal winter over the MC

Monthly mean and MJO-cycle water budget variations are related strongly to P and C in all domains. The LWUR also shows large differences between domains, and it is highest over BOL compared with other domains. It is therefore likely that evaporation and evapotranspiration contribute more to precipitation over BOL. However, the diurnal cycle in precipitation is most pronounced over islands and coastal regions compared with other time scales. It is therefore necessary to consider the water budget on a diurnal time scale over these regions.

To elucidate further the diurnal cycle of the water budget over the MC, Fig. 7 shows anomalies from the daily NDJFM mean at 0000 and 1200 UTC for precipitation, vertically integrated moisture flux vectors, and convergence. These times correspond roughly to the morning and evening over the MC, respectively. Diurnal precipitation and moisture flux convergence cycles are clear over land (BOL and NGL) and coastal regions (BOC and NGC). The diurnal precipitation cycle is also pronounced with late afternoon to evening maxima over land and nighttime to morning maxima over the surrounding sea areas. The moisture flux convergence cycle, dominated by the low-level wind field at 850 hPa, is related to the land–sea breeze and is most prominent on islands and coastal regions. Moisture flux convergence is also enhanced over land in the afternoon to evening, and over the surrounding ocean in the nighttime to morning period.

The diurnal fluctuations of precipitation and moisture flux convergence are less pronounced over the MCO than other regions throughout the day. The water budget over BO and NG is dominated by a diurnal time scale, which is restricted to the island and its surrounding oceans. Concerning the moisture flux convergence balance at a diurnal time scale, some cancellations emerge; for example, moisture flux convergence and divergence cancel each other out throughout the course of the day over BO and NG (Figs. 7c,d). Thus, a seasonal, that is, daily mean time scale moisture flux convergence is not evident over BO (Figs. 1b,d). In contrast, the seasonal march of precipitation and moisture flux convergence is pronounced over NG because of the migration of the seasonal cycle of the ITCZ (Fig. 1). Hence, the diurnal time scale variation is dominant over BO, while both the diurnal and daily mean time scale variations are dominant over NG.

The spatial distributions of diurnal precipitation and moisture flux convergence associated with the MJO have similar patterns to the seasonal mean over the MC (figure not shown). Moisture flux convergence over BO, in particular, does not reflect the effect of the MJO (Fig. 5); however, the diurnal cycles of precipitation and moisture flux convergence are clear and in phase.

e. *Effect of the diurnal atmospheric water cycle associated with the MJO*

The daily mean and the diurnal variation of the hydrologic cycle over the MC were described in the previous subsections. Here, to investigate the relationship between the precipitation and convection systems of those time scales, composite height–longitude diagrams of the daily mean vertical velocity anomalies and their diurnal variance averaged between 5°S and 5°N (including BO in the active and break phases) are shown in Fig. 8. This figure represents the deep convective systems, which have low-level convergence at 700 hPa and strong upward motions from ~700 to 200 hPa in both time scales. In active phases, the daily mean time scale upward motion centered on 300 hPa, associated with the MJO convection, is strengthened and propagates from the Indian Ocean to the MC (see Salby and Hendon 1994; Zhang and Hendon 1997). In break phases, the downward motion, also associated with MJO convection, moves eastward from the MC to the central Pacific. On the diurnal time scale, the upward motion related to convective activity is distinct over the islands and coastal regions of Borneo (120°E) and Sumatra (100°E) in both phases. Notable vertical velocity variability does not occur over the ocean in either active or break phases. The vertical velocity variability is amplified, and it becomes widespread over land and the surrounding oceans in the active phase, while it can be seen in only limited regions over the islands in break phases. It should be noted that in the break phase, the land–sea breeze and the localized mountain–valley circulation in the interior of BO have been reported to become obvious compared with the active phase (Kanamori et al. 2013). The relationship between the MJO and the diurnal convection cycle is similar over BO and NG in both phases (figure not shown).

To examine the impact of the relationship between moisture transport of the MJO and diurnal time scales of the water budget over the MC, we split the water vapor transport into rotational and divergent components. The moisture flux potential component roughly approximates a moisture source and sink (Chen et al. 1995). Figure 9 shows the composite of the moisture flux potential and the diurnal variance of the moisture flux potential associated with the two MJO phases. The daily mean moisture fluxes tend to converge (diverge) in the active (break) phase of the MJO over the MC. However, we should note that there is strong diurnal variance of the moisture flux potential around Sumatra, BO, and NG in both phases. This implies that the diurnal time scale of a moisture source and sink plays an important role in maintaining precipitation over the islands, for example, BO and NG, despite MJO modulation. Both daily mean and diurnal time scales, therefore, have distinct influences on the water budget over the MC, and the effects of diurnal variations in moisture transport are especially important for the water budget of the land and coastal regions of both BO and NG.

5. Discussion and conclusions

Hydrologic cycles over the MC could be classified into land and ocean areas using land–ocean mask data and then into coastal and ocean regions based on the diurnal variance in precipitation. The hydrologic cycles over the land (BOL and NGL) and coastal regions (BOC and NGC) of two major island regions (BO and NG) are linked because of the influence of the land–sea breeze. The seasonal change in moisture flux transport associated with the large-scale circulation is smaller over BO than over other regions (NG and MCO). The seasonal cycle of the atmospheric water budget shows that precipitation is synchronized with moisture flux convergence over all of the study regions. The cycle is relatively weaker over BO and MCO compared with NG. Parameter C does not contribute much to precipitation over the BOL region in comparison with LWUR, which does make a significant contribution to evapotranspiration throughout the year (~85% of the annual mean). Based on in situ observations, the LWUR was found to range

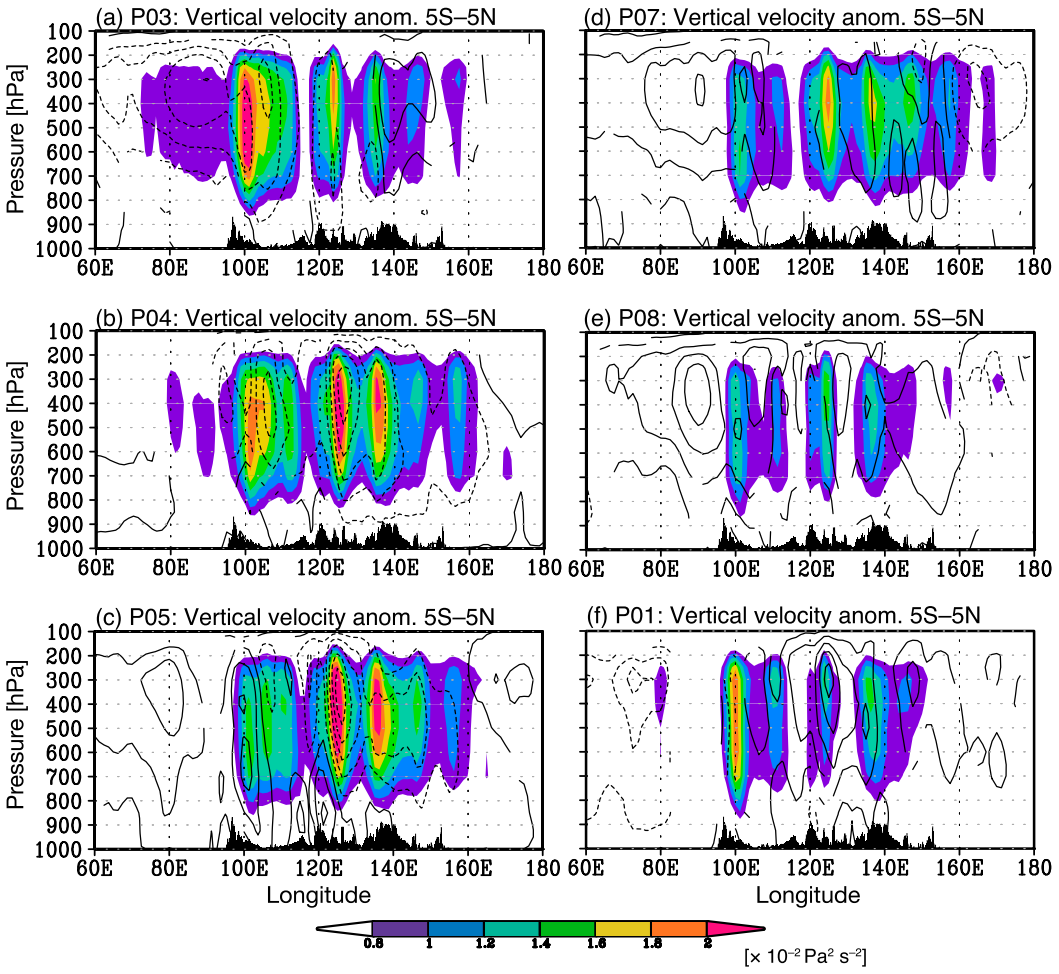

FIG. 8. Composite vertical–longitude diagrams of vertical velocity potential anomalies (contours) and their diurnal variance (shaded areas) averaged between 5°S and 5°N in (a)–(c) peak active and (d)–(f) break phases. These anomalies show the difference from the seasonal mean (NDJFM). Black shading along the bottom of the figures denotes topography. The solid (dashed) contours show positive (negative) values. The contour interval is 1×10^{-2} Pa s^{-1}, from -5 to 4×10^{-2} Pa s^{-1}. Contours and shading are plotted only if significant at the 95% confidence level.

between 74% (Kumagai et al. 2005) and 50% (Kume et al. 2011) in western BO. The regional mean LWUR over BOL is overestimated in comparison with results obtained using ground-based observations (~50%–75%) that are consistent with the atmospheric water budget calculations in this study. In NGL, the LWUR is small because P depends on C in the wet season (NDJFM). The LWUR also makes a relatively small contribution to the atmospheric water budget over the MC.

The diurnal variability in precipitation, moisture flux, and divergence is clearly pronounced over land and coastal regions over both major islands (BO and NG). The diurnal variation in precipitation is generated by land–sea temperature contrasts and the resulting land–sea breeze convection systems over the MC (Houze et al. 1981; Nitta and Sekine 1994; Kikuchi and Wang 2008; Biasutti et al. 2012). The land surface heating process generates sea breezes and thermal convection over the land from afternoon to evening. Also, from midnight to morning, land breezes cause low-level convergence and precipitation over coastal regions (e.g., Yang and Slingo 2001; Houze et al. 1981; Nitta and Sekine 1994; Kanamori et al. 2013). The diurnal cycle of low-level wind circulation appears because of the thermal contrast between the land and surrounding oceans (see Fig. 7). On the diurnal time scale, between BO and NG, the thermal contrasts differ little and the anomalies of the low-level wind circulation are similar. Moisture flux divergence (convergence) occurs from afternoon to night (from midnight to morning) over coastal regions in BO and NG. It appears that the contributions of moisture flux convergence and divergence to precipitation, particularly over BO, balance

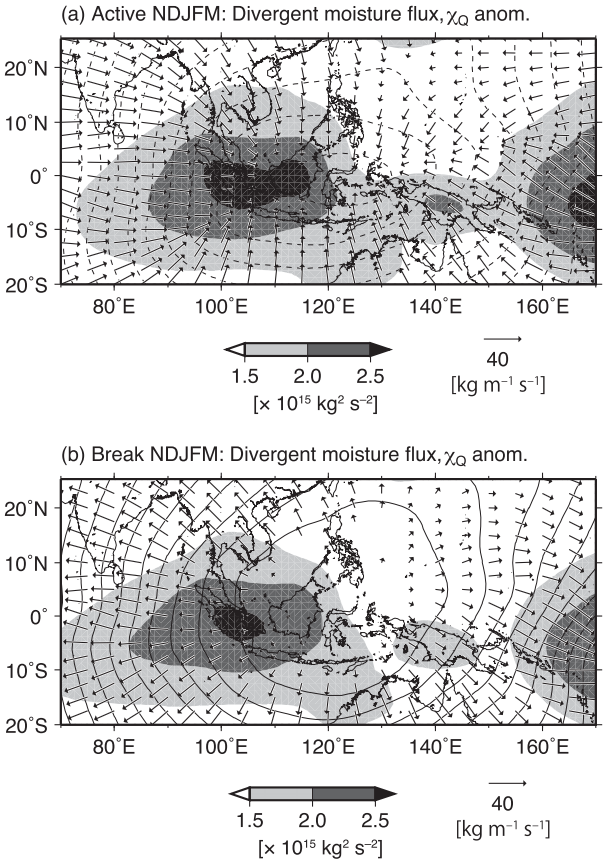

FIG. 9. Composite anomalies of the vertically integrated moisture flux potential ($kg\,m^{-1}\,s^{-1}$; contours) and divergent moisture flux vectors ($kg\,m^{-1}\,s^{-1}$) of vertically integrated moisture fluxes in peak (a) active and (b) break phases. These anomalies show the difference from the seasonal mean (NDJFM). The shading also indicates the composite variance in the diurnal component of the moisture flux potential between both phases. The solid (dashed) contours show positive (negative) values. The contour interval is $1 \times 10^8\,kg\,s^{-1}$, from -1.2 to $1.3 \times 10^8\,kg\,s^{-1}$. Vectors, contours, and shading are plotted only if significant at the 95% confidence level.

out throughout the day. Over BO, the large-scale circulation has weak influence on the seasonal water budget, but the localized low-level circulation has strong influence on the hydrologic cycle on diurnal time scales. Seasonal and diurnal processes dominate the variability in the hydrologic cycle over NG. Furthermore, the hydrologic cycle of MCO depends mostly on seasonal variations. Thus, the diurnal cycle plays an important role in the exchange of water between island and coastal regions across the MC.

This study also investigated the impact of the MJO, a dominant mode of deep convection and heavy precipitation, on the hydrologic cycle of the MC. Precipitation and moisture flux convergence are modulated by the propagating MJO disturbance. This impact appears strongest in the MCO, and it is more pronounced in coastal areas (BOC and NGC) in comparison with land areas (BOL and NGL). The MJO is propagated preferentially over the ocean between the MC and Australian continent. During its passage over the MC, topographic blocking of the MJO reduces its impact on precipitation over the land (i.e., BO) in comparison with the oceans (Hsu and Lee 2005; Wu and Hsu 2009). The topographic configuration of NG is elongated in the east–west direction and narrow in the north–south direction. Therefore, when the MJO transits, precipitation/convection activities should be enhanced over NGC. Note that the diurnal cycle of precipitation/convection is pronounced over both BO and NG in the active phase of the MJO (Ichikawa and Yasunari 2008, 2006; Kanamori et al. 2013). Additionally, the LWUR does not show any variation associated with MJO.

The diurnal variation in the MC atmospheric hydrologic cycle associated with the MJO is characterized by enhanced moisture flux convergence from midnight to morning over coastal regions, from the active to break phases of the MJO. The low-level wind anomaly in the active phase increases this convergence, producing heavy precipitation around midnight over coastal regions (Kanamori et al. 2013). The diurnal cycle of convection and precipitation in both phases is differentiated clearly between land and coastal regions. Moisture flux convergence and divergence over BO and NG is also modulated on diurnal time scales; therefore, the effect of diurnal variation on moisture transport is especially important in the hydrologic cycle over these regions.

The effect of local-scale diurnal variations on the atmospheric hydrologic cycle is larger over BO than over NG. The atmospheric water cycle over NG depends on both large-scale (i.e., the MJO) and local-scale (e.g., land–sea breeze) variations. The modulation of diurnal precipitation by MJO disturbances is smaller over BOL (Kanamori et al. 2013) and larger over NGL (Ichikawa and Yasunari 2008). Over NG, the diurnal precipitation cycle is enhanced over the southwestern part of the island in the break phase of the MJO, but over southwestern and northeastern parts of island, it is enhanced during the active phase of the MJO (Ichikawa and Yasunari 2008). It is assumed that the shapes (including orography) of the islands generate different hydrologic cycles in BO and NG.

The atmospheric water cycle in BO is restricted spatially to land and coastal areas. Moisture transport from coastal areas, caused by the land–sea breeze, is a source of the precipitation over coastal land in the afternoon. Furthermore, the sea breeze transports moisture from evaporation in coastal and land areas to interior areas of the land. This evaporation might contribute to the

night–midnight precipitation over interior land areas. Note that the effect of moisture transport from coastal areas is small over BO because of the cancellation of terms of the hydrologic budget due to the diurnal land–sea breeze cycle. The LWUR is therefore high over BO compared with other regions. Evapotranspiration from the surface (tropical rain forest) plays a major role in the maintenance of the high levels of precipitation over BO, and it increases the LWUR over BOL. Kumagai et al. (2005) suggested that most precipitation is recycled from terrestrial evapotranspiration over BOL. The effect of evapotranspiration on the hydrologic cycle at this time scale could not be estimated accurately in this work because local solar time over the MC does not correspond to the 6-h reanalysis data.

The different characteristics of the hydrologic cycles of the major islands (BO and NG) are concluded as follows:

1) Migration of the ITCZ and enhancement of the SPCZ both affect the seasonal changes of precipitation and moisture flux convergence more strongly over NG than over BO in boreal winter, mainly attributed to their latitudinal differences in location within the MC.
2) Large-scale disturbances associated with the MJO enhance the precipitation as well as the moisture flux convergence over the oceans surrounding both islands.
3) The impact of the MJO is small over land where there is topographic blocking (i.e., BO), and it is larger over NGL than BOL because of their different shapes.
4) The diurnal cycles of precipitation and moisture flux convergence, which are characterized by land–ocean and mountain–valley thermal contrasts, are pronounced both in active and break phases of the MJO over BOL and NGL.
5) Findings 1–4 result in diurnal, MJO, and seasonal time scales having important roles in the hydrologic cycle in NG, whereas the diurnal time scale is most dominant in the hydrologic cycle over BO. Furthermore, evapotranspiration might contribute considerably to the hydrologic cycle over BO because the effects of large-scale seasonal and intraseasonal circulations are smaller in comparison with NG.

Given that rain forests are a major driver of the hydrologic cycle, changes in forest cover can affect the atmospheric water balance (Bonan 2008; Aragão 2012). Modeling work has illustrated the effects of deforestation on both the decrease (Kanae et al. 2001; Yasunari et al. 2006; Takahashi et al. 2017) and the increase (Spracklen et al. 2012) in local precipitation. It is therefore an important challenge for future research to estimate the evapotranspiration in Borneo over several time scales. In addition, the diurnal cycles of precipitation and convection in reanalysis data must be used with caution because convective parameterizations employed by global reanalysis data have a quick trigger that initiates weak convection in the afternoons over land despite the supply of moisture for the observed precipitation maxima (Ruane and Roads 2007). A numerical simulation using regional and cloud-resolving models would help further the understanding of these processes.

Acknowledgments. This work was supported by a Grant-in-Aid for Scientific Research (25281005) and grants for the Program for Risk Information on Climate Change' project provided by the Ministry of Education, Science and Culture, Japan. This study was also conducted with support from the Japan Society for the Promotion of Science (JSPS) KAKENHI Grant 17H01477 and 15H02645. This paper is part of the Ph.D. thesis of H. Kanamori (Kanamori 2015). The authors thank Dr. H. Masunaga for invaluable comments and suggestions.

REFERENCES

Aragão, L. E. O. C., 2012: The rainforest's water pump. *Nature*, **489**, 217–218, https://doi.org/10.1038/nature11485.

Biasutti, M., S. E. Yuter, C. D. Burleyson, and A. H. Sobel, 2012: Very high resolution rainfall patterns measured by TRMM precipitation radar: Seasonal and diurnal cycles. *Climate Dyn.*, **39**, 239–258, https://doi.org/10.1007/s00382-011-1146-6.

Bonan, G. B., 2008: Forests and climate change: Forcings, feedbacks, and the climate benefits of forests. *Science*, **320**, 1444–1449, https://doi.org/10.1126/science.1155121.

Chang, C. P., P. A. Harr, and H. J. Chen, 2005a: Synoptic disturbances over the equatorial South China Sea and western Maritime Continent during boreal winter. *Mon. Wea. Rev.*, **133**, 489–503, https://doi.org/10.1175/MWR-2868.1.

——, Z. Wang, J. McBride, and C. H. Liu, 2005b: Annual cycle of Southeast Asia–Maritime Continent rainfall and the asymmetric monsoon transition. *J. Climate*, **18**, 287–301, https://doi.org/10.1175/JCLI-3257.1.

Chen, T. C., and K. Takahashi, 1995: Diurnal variation of outgoing longwave radiation in the vicinity of the South China Sea: Effect of intraseasonal oscillation. *Mon. Wea. Rev.*, **123**, 566–577, https://doi.org/10.1175/1520-0493(1995)123<0566:DVOOLR>2.0.CO;2.

——, J. M. Chen, and J. Pfaendtner, 1995: Low-frequency variations in the atmospheric branch of the global hydrological cycle. *J. Climate*, **8**, 92–107, https://doi.org/10.1175/1520-0442(1995)008<0092:LFVITA>2.0.CO;2.

Goessling, H. F., and C. H. Reick, 2011: What do moisture recycling estimates tell us? Exploring the extreme case of non-evaporating continents. *Hydrol. Earth Syst. Sci.*, **15**, 3217–3235, https://doi.org/10.5194/hess-15-3217-2011.

Hendon, H. H., and M. L. Salby, 1994: The life cycle of the Madden–Julian oscillation. *J. Atmos. Sci.*, **51**, 2225–2237, https://doi.org/10.1175/1520-0469(1994)051<2225:TLCOTM>2.0.CO;2.

Hidayat, R., and S. Kizu, 2010: Influence of the Madden-Julian oscillation on Indonesian rainfall variability in austral summer. *Int. J. Climatol.*, **30**, 1816–1825, https://doi.org/10.1002/joc.2005.

Houze, R. A., S. G. Geotis, F. D. Marks, and A. K. West, 1981: Winter monsoon convection in the vicinity of north Borneo. Part I: Structure and time variation of the clouds and precipitation. *Mon. Wea. Rev.*, **109**, 1595–1614, https://doi.org/10.1175/1520-0493(1981)109<1595:WMCITV>2.0.CO;2.

Hsu, H. H., and M. Y. Lee, 2005: Topographic effects on the eastward propagation and initiation of the Madden-Julian oscillation. *J. Climate*, **18**, 795–809, https://doi.org/10.1175/JCLI-3292.1.

Huffman, G. J., and Coauthors, 2007: The TRMM Multisatellite Precipitation Analysis (TMPA): Quasi-global, multiyear, combined-sensor precipitation estimates at fine scales. *J. Hydrometeor.*, **8**, 38–55, https://doi.org/10.1175/JHM560.1.

Ichikawa, H., and T. Yasunari, 2006: Time–space characteristics of diurnal rainfall over Borneo and surrounding oceans as observed by TRMM-PR. *J. Climate*, **19**, 1238–1260, https://doi.org/10.1175/JCLI3714.1.

——, and ——, 2007: Propagating diurnal disturbances embedded in the Madden-Julian oscillation. *Geophys. Res. Lett.*, **34**, L18811, https://doi.org/10.1029/2007GL030480.

——, and ——, 2008: Intraseasonal variability in diurnal rainfall over New Guinea and the surrounding oceans during austral summer. *J. Climate*, **21**, 2852–2868, https://doi.org/10.1175/2007JCLI1784.1.

Iguchi, T., T. Kozu, R. Meneghini, J. Awaka, and K. Okamoto, 2000: Rain-profiling algorithm for the TRMM precipitation radar. *J. Appl. Meteor.*, **39**, 2038–2052, https://doi.org/10.1175/1520-0450(2001)040<2038:RPAFTT>2.0.CO;2.

Kanae, S., T. Oki, and K. Musiake, 2001: Impact of deforestation on regional precipitation over the Indochina Peninsula. *J. Hydrometeor.*, **2**, 51–70, https://doi.org/10.1175/1525-7541(2001)002<0051:IODORP>2.0.CO;2.

Kanamori, H., 2015: Climatological study on atmospheric water cycling over Maritime Continent. Ph.D. thesis, Nagoya university, 95 pp.

——, T. Yasunari, and K. Kuraji, 2013: Modulation of the diurnal cycle of rainfall associated with the MJO observed by a dense hourly rain gauge network at Sarawak, Borneo. *J. Climate*, **26**, 4858–4875, https://doi.org/10.1175/JCLI-D-12-00158.1.

Kikuchi, K., and B. Wang, 2008: Diurnal precipitation regimes in the global tropics. *J. Climate*, **21**, 2680–2696, https://doi.org/10.1175/2007JCLI2051.1.

Kumagai, T., and Coauthors, 2005: Annual water balance and seasonality of evapotranspiration in a Bornean tropical rainforest. *Agric. For. Meteor.*, **128**, 81–92, https://doi.org/10.1016/j.agrformet.2004.08.006.

——, H. Kanamori, and T. Yasunari, 2013: Deforestation-induced reduction in rainfall. *Hydrol. Processes*, **27**, 3811–3814, https://doi.org/10.1002/hyp.10060.

Kume, T., N. Tanaka, K. Kuraji, H. Komatsu, N. Yoshifuji, T. M. Saitoh, M. Suzuki, and T. Kumagai, 2011: Ten-year evapotranspiration estimates in a Bornean tropical rainforest. *Agric. For. Meteor.*, **151**, 1183–1192, https://doi.org/10.1016/j.agrformet.2011.04.005.

Madden, R. A., and P. R. Julian, 1994: Observations of the 40–50-day tropical oscillation—A review. *Mon. Wea. Rev.*, **122**, 814–837, https://doi.org/10.1175/1520-0493(1994)122<0814:OOTDTO>2.0.CO;2.

Mori, S., H. Jun-Ichi, Y. I. Tauhid, and M. D. Yamanaka, 2004: Diurnal land–sea rainfall peak migration over Sumatera Island, Indonesian Maritime Continent, observed by TRMM satellite and intensive rawinsonde soundings. *Mon. Wea. Rev.*, **132**, 2021–2039, https://doi.org/10.1175/1520-0493(2004)132<2021:DLRPMO>2.0.CO;2.

Neale, R., and J. Slingo, 2003: The Maritime Continent and its role in the global climate: A GCM study. *J. Climate*, **16**, 834–848, https://doi.org/10.1175/1520-0442(2003)016<0834:TMCAIR>2.0.CO;2.

Nitta, T., and S. Sekine, 1994: Diurnal variation of convective activity over the tropical western Pacific. *J. Meteor. Soc. Japan*, **72**, 627–641, https://doi.org/10.2151/jmsj1965.72.5_627.

Ohsawa, T., H. Ueda, T. Hayashi, A. Watanabe, and J. Matsumoto, 2001: Diurnal variations of connective activity and rainfall in tropical Asia. *J. Meteor. Soc. Japan*, **79**, 333–352, https://doi.org/10.2151/jmsj.79.333.

Onogi, K., and Coauthors, 2007: The JRA-25 reanalysis. *J. Meteor. Soc. Japan*, **85**, 369–432, https://doi.org/10.2151/jmsj.85.369.

Ramage, C. S., 1968: Role of a tropical "maritime continent" in atmospheric circulation. *Mon. Wea. Rev.*, **96**, 365–370, https://doi.org/10.1175/1520-0493(1968)096<0365:ROATMC>2.0.CO;2.

Rauniyar, S. P., and K. J. E. Walsh, 2011: Scale interaction of the diurnal cycle of rainfall over the Maritime Continent and Australia: Influence of the MJO. *J. Climate*, **24**, 325–348, https://doi.org/10.1175/2010JCLI3673.1.

Ruane, A. C., and J. O. Roads, 2007: The diurnal cycle of water and energy over the continental United States from three reanalyses. *J. Meteor. Soc. Japan*, **85A**, 117–143, https://doi.org/10.2151/jmsj.85A.117.

——, and ——, 2008: Dominant balances and exchanges of the atmospheric water cycle in the Reanalysis 2 at diurnal, annual, and intraseasonal time scales. *J. Climate*, **21**, 3951–3966, https://doi.org/10.1175/2007JCLI2015.1.

Salby, M. L., and H. H. Hendon, 1994: Intraseasonal behavior of clouds, temperature, and motion in the tropics. *J. Atmos. Sci.*, **51**, 2207–2224, https://doi.org/10.1175/1520-0469(1994)051<2207:IBOCTA>2.0.CO;2.

Spracklen, D. V., S. R. Arnold, and C. M. Taylor, 2012: Observations of increased tropical rainfall preceded by air passage over forests. *Nature*, **489**, 282–285, https://doi.org/10.1038/nature11390.

Takahashi, A., T. Kumagai, H. Kanamori, H. Fujinami, T. Hiyama, and M. Hara, 2017: Impact of tropical deforestation and forest degradation on precipitation over Borneo island. *J. Hydrometeor.*, **18**, 2907–2922, https://doi.org/10.1175/JHM-D-17-0008.1.

Tian, B. J., D. E. Waliser, and E. J. Fetzer, 2006: Modulation of the diurnal cycle of tropical deep convective clouds by the MJO. *Geophys. Res. Lett.*, **33**, L20704, https://doi.org/10.1029/2006GL027752.

Trenberth, K. E., and C. J. Guillemot, 1995: Evaluation of the global atmospheric moisture budget as seen from analyses. *J. Climate*, **8**, 2255–2272, https://doi.org/10.1175/1520-0442(1995)008<2255:EOTGAM>2.0.CO;2.

van der Ent, R. J., and H. H. G. Savenije, 2011: Length and time scales of atmospheric moisture recycling. *Atmos. Chem. Phys.*, **11**, 1853–1863, https://doi.org/10.5194/acp-11-1853-2011.

Waliser, D. E., B. J. Tian, X. S. Xie, W. T. Liu, M. J. Schwartz, and E. J. Fetzer, 2009: How well can satellite data characterize the water cycle of the Madden-Julian oscillation? *Geophys. Res. Lett.*, **36**, L21803, https://doi.org/10.1029/2009GL040005.

Wheeler, M. C., and H. H. Hendon, 2004: An all-season real-time multivariate MJO index: Development of an index for monitoring and prediction. *Mon. Wea. Rev.*, **132**, 1917–1932, https://doi.org/10.1175/1520-0493(2004)132<1917:AARMMI>2.0.CO;2.

Wu, C. H., and H. H. Hsu, 2009: Topographic influence on the MJO in the Maritime Continent. *J. Climate*, **22**, 5433–5448, https://doi.org/10.1175/2009JCLI2825.1.

Yang, G. Y., and J. Slingo, 2001: The diurnal cycle in the tropics. *Mon. Wea. Rev.*, **129**, 784–801, https://doi.org/10.1175/1520-0493(2001)129<0784:TDCITT>2.0.CO;2.

Yasunari, T., K. Saito, and K. Takata, 2006: Relative roles of large-scale orography and land surface processes in the global hydroclimate. Part I: Impacts on monsoon systems and the tropics. *J. Hydrometeor.*, **7**, 626–641, https://doi.org/10.1175/JHM515.1.

Zhang, C. D., and H. H. Hendon, 1997: Propagating and standing components of the intraseasonal oscillation in tropical convection. *J. Atmos. Sci.*, **54**, 741–752, https://doi.org/10.1175/1520-0469(1997)054<0741:PASCOT>2.0.CO;2.

Zhou, L., and Y. Q. Wang, 2006: Tropical rainfall measuring mission observation and regional model study of precipitation diurnal cycle in the New Guinean region. *J. Geophys. Res.*, **111**, D17104, https://doi.org/10.1029/2006JD007243.